

PAPER**ANTHROPOLOGY**

Brian J. Powell,¹ B.S.; Nicholas V. Passalacqua,² M.S.; Timothy G. Baumer,¹ M.S.; Todd W. Fenton,² Ph.D.; and Roger C. Haut,¹ Ph.D.

Fracture Patterns on the Infant Porcine Skull Following Severe Blunt Impact*

ABSTRACT: The objective of this study was to document patterns of fracture on infant porcine skulls aged 2–28 days ($n = 57$) because of a single, high energy blunt impact to the parietal bone with rigid (nondeformable) and compliant (deformable) interfaces. Fracture patterns were mapped using Geographic Information System software. For the same generated impact force, the rigid interface produced more fractures than the compliant interface for all ages. This study also showed that this increased level of impact energy versus an earlier study using a lower energy resulted in new sites of fracture initiation and also caused previously defined fractures that propagate into an adjacent bone. Several unique characteristics of bone and diastatic fracture were documented as a function of specimen age, impact energy, and interface. These data describe some baseline characteristics of skull fracture using an animal model that may help guide future studies from forensic case files.

KEYWORDS: forensic science, skull fracture, infant, porcine, impact energy, interface effect, age effect, Geographic Information System

Determining whether a head injury to an infant was the result of abuse or an accident is a common problem in forensic investigations. Typically, the legal system depends on the testimony of medical experts to determine whether the force imparted to a head in a given scenario is consistent with a specific fracture pattern, even though there may be little scientific basis for their conclusions. While head injuries account for 80% of fatal child abuse in young children (1), distinguishing between accidental and abusive trauma can be difficult, as both may produce similar types of skull fractures (2). Linear, complex, and depressed skull fractures have been documented in both cases (3,4). The most commonly fractured cranial bone in both accidental and abuse cases is the parietal (5–7). And to further complicate the problem, the risk of head injury is also dependent on the contacting surface (8). Other variables, such as the area struck, thickness of the skull, thickness of the scalp and hair, and impact direction, have been shown to affect the pattern of skull fracture in forensic cases (9,10). However, primarily because of limited availability and ethical issues, little has been done to date in establishing a solid scientific basis for determining the causation of impact head injuries based on fracture pattern using the human infant cadaver surrogate.

Because scaling of the adult skull has met with limited success in predicting the impact response of the pediatric skull (11), an animal model has recently displayed utility in the study of human pediatric head injury: the immature porcine model. This animal model has

been used to predict, for example, fracture forces for the human pediatric femur (12) and strain in the braincase and sutures (13). Studies by this laboratory (14) and others (15) have also established correlations between the mechanical properties of developing human cranial bone and suture versus those of the immature porcine model. A more recent study by Baumer et al. (16) investigated the effects of impact interface stiffness (deformability) and specimen age (up to 28 days) using an infant porcine model on the location of fracture initiation in the parietal bone and adjacent sutures. One result from the study is that relatively low energy impacts typically initiate bone fracture at specific sites along the bone-suture boundary in this animal model. However, in many pediatric death cases there are multiple skull fractures that sometimes are shown to extend across suture boundaries and into adjacent, seemingly unimpacted bones (6,17). Multiple, wide, or cross-suture fractures are typically thought to be indicative of high energy trauma (5). It was therefore necessary for our laboratory to study the effect of higher energy impacts on our animal model that may be more representative of the situation often documented in current forensic case files.

There were two hypotheses investigated in the current study. First, we hypothesized that the locations of fracture would not vary for a doubling of the impact energy from the initiation sites documented by Baumer et al., in 2010 (16). Second, we hypothesized that a doubled impact energy would simply increase the length of fractures via propagation for all ages and that this means of energy dissipation would be the same for both rigid and compliant interfaces. These data may then help in a more complete documentation of this animal model of the human infant and in the understanding of the effects of impact energy, impact interface, and specimen age on more complex fracture patterns in this model.

Materials and Methods

Porcine specimens were received from a local supplier and stored at -20°C . A total of 57 specimens (aged 2–28 days) were

¹Orthopaedic Biomechanics Laboratories, College of Osteopathic Medicine, Michigan State University, A-407 East Fee Hall, East Lansing, MI 48824.

²Department of Anthropology, College of Social Sciences, Michigan State University, East Lansing, MI 48824.

*Funded by the National Institute of Justice, Office of Justice Programs, United States Department of Justice (2007-DN-BX-K196). The opinions, findings, and conclusions expressed in this publication are those of the authors and do not necessarily reflect the views of the Department of Justice.

Received 22 Mar. 2010; and in revised form 21 Sept. 2010; accepted 30 Dec. 2010.

used for this study. The animals died of natural causes and were frozen within 12 h of death. All specimens were free of head injury, which was confirmed during preparation.

The test procedure was described in a previous study (16). Briefly, the head was allowed to thaw at room temperature for 24 h before the scalp and facial tissues on the left side were removed. The removal of these tissues allowed the specimens to be transversely and rotationally constrained in a bed of air-hardened epoxy (Fibre Strand; Martin Senour Corp., Cleveland, OH). Phosphate-buffered saline solution was applied regularly during the preparation. The specimen was placed in a four degree of freedom fixture that allowed adjustments of the impact site (Fig. 1). The skull was oriented such that the center of the right parietal bone was normal to the impact interface.

The specimens were impacted using a gravity accelerated mass (GAM) (Fig. 2). A single impact was delivered using an operational amplifier comparator circuit to monitor the impact force and energize an electromagnetic solenoid to catch the GAM immediately after the impact force returned to zero. The forces were recorded using a load transducer (4.45 kN capacity, model AL311CV; Sensotec, Columbus, OH) mounted immediately behind the impact interface. The force data were sampled at 10,000 Hz. Two interfaces were used in this study: rigid and compliant. The rigid interface was a solid aluminum cylinder with *c.* 16 cm² of

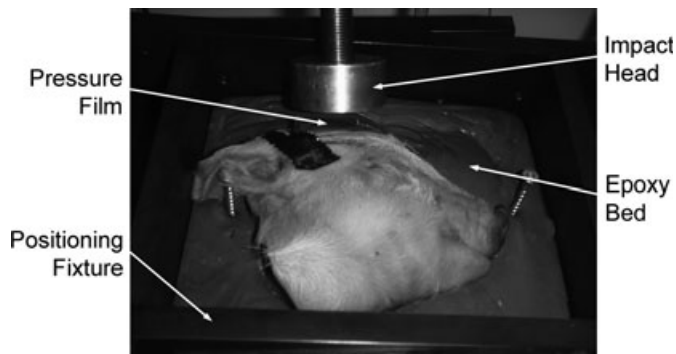


FIG. 1—Orientation of the right parietal bone with rigid impact interface.

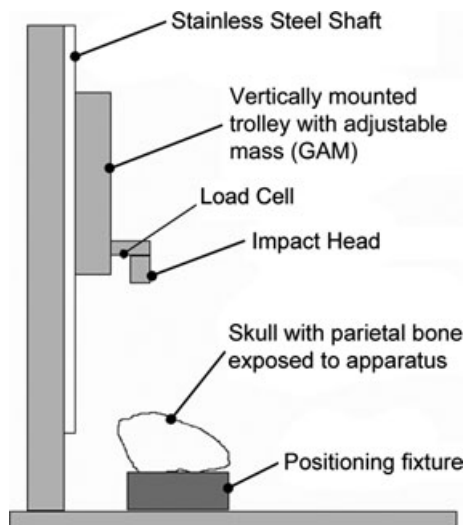


FIG. 2—The drop tower with gravity accelerated mass shown.

surface area (Fig. 1). The compliant interface was a deformable aluminum block (1.10 MPa crush strength Hexcel; Hexcel Corp., Stamford, CT), *c.* 3 cm thick with a 16 cm² surface area, attached to the rigid interface.

Impact energy was controlled by varying the drop height of a 1.67 kg GAM. A slightly larger, 1.92 kg mass was used to generate fracture in specimens aged 21 days and older. The mass of the impact interface was included in the GAM. Energy levels for each age were double those of a previous study (16). The impact energy was doubled by raising the height of the GAM to twice the height of the previous study. The input energy for the compliant and rigid interfaces was equal at each age.

Pressure-sensitive film packets (Prescale; Fuji Film Ltd., Tokyo, Japan) were attached to the impact site of each specimen to capture contact area. Two sheets of polyethylene were used to protect low (0–10 MPa)- and medium (10–50 MPa)-range pressure films stacked on top of one another from fluids (18). The medium pressure film data was not used in the current study as the impact pressures were too low to record on the film.

After impact, the remaining periosteum and soft tissues were removed from the skull, and it was visually inspected for bone fracture and suture damage. The remaining soft tissue on the skull was then removed after the skull was gently cooked in a bath of water, without chemicals, until the soft tissues could be easily removed. After glueing the skull back together, the length of skull fractures was measured to the nearest millimeter using a soft, flexible measuring tape, which contoured to the curvature of the skull. Complete fracture diagrams were constructed manually for each specimen.

To compare the patterns of fracture between specimens and interfaces, a Geographic Information System (GIS) method was utilized in the study. The pattern of fracture from each skull was constructed using a projected view of the porcine cranium that best highlighted the right side of the skull with fracture configurations superimposed on it for each specimen. A second view of the posterior aspect of the cranium was also included as many high energy fractures involved the occipital bone. Fracture data from Baumer et al. (16) were also revisited to compare low energy rigid and compliant fracture configurations to the current study. Porcine specimens were separated into two different age groups (2–9 and 19–28 days) for both the rigid and compliant impact interfaces and at low and high energy levels to better demonstrate the fracture pattern changes in relation to porcine growth and development, impact interface, and input energy. These age groups were chosen based on general observations of gross fracture and material property changes for the skull and suture tissues documented in the literature (14,16). The fracture pattern for each porcine cranium was traced into individual shape files (19). The GIS model then counted overlaid fracture patterns on each cranium, generating a map of where fractures appeared most frequently. After each map was constructed, the GIS model was used to discuss the differences in fracture patterns between specimens of different age, impact energy, and interface.

The impact data were analyzed for age effects using linear regression analyses. Comparisons between the interfaces were performed using a two-factor (age, interface) analysis of variance (ANOVA). Statistically significant effects were reported for $p < 0.05$.

Results

Impact energies were doubled from those used by Baumer et al. (16) by doubling the drop height at each age. The drop heights ranged from 0.2 m for a 2-day-old specimen to 1.2 m for a

28-day-old specimen. The values of impact energy ranged from 3.1 to 22.6 J, respectively.

The impact force on the skulls increased with age for both interfaces, and there was little difference in the peak impact force (within 100 N at a given age) between the two interfaces (Fig. 3). Linear regression analysis indicated a significant increase in the impact force with age for the compliant ($p < 0.001$) and the rigid interfaces ($p = 0.006$).

Due primarily to the increase in impact force applied to the skull, the contact areas generated during impact were found to significantly increase ($p = 0.003$) with age at a similar rate for both interfaces (Fig. 4). A two-factor ANOVA (age, interface) for the contact area showed a significantly larger area of contact generated with the compliant than rigid interface.

The length of fracturing (in bone and along sutures) versus age plot showed, on average, a significantly larger ($p = 0.034$) amount of fracturing for the rigid than the compliant interfaces (Fig. 5).

The GIS fracture maps confirmed that the length of fractures was greater for rigid than compliant interface impacts for the younger age group in the current study (Fig. 6a,b). For the compliant interface experiments, the pattern maps showed fractures primarily appearing to initiate at four sites adjacent to the sutures along the perimeter of the parietal bone. However, for the rigid, there appeared to be numerous initiation sites. There was also

significantly more diastatic fracturing in the rigid than compliant interface experiments, specifically along the coronal suture.

In the older group of specimens (19–28 days), more fracturing was again confirmed for the rigid than compliant interface experiments (Fig. 7a,b). Yet, in these experiments, no diastatic fractures were noted. Sites of fracture initiation were evident in the parietal bone along the coronal and lambdoid sutures for the compliant interface experiments. Two of these sites were similar to those

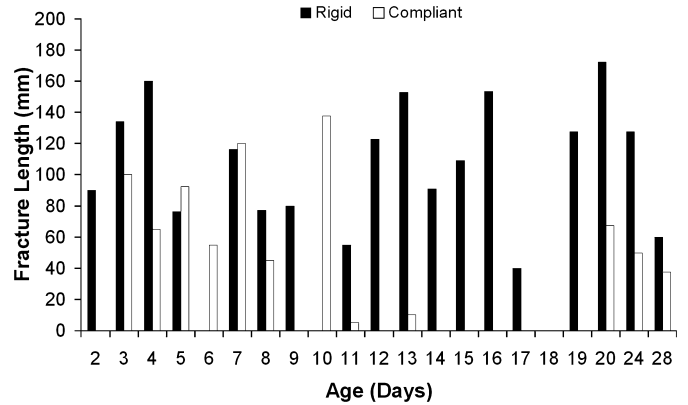


FIG. 5—The length of total skull fracture as a function of age.

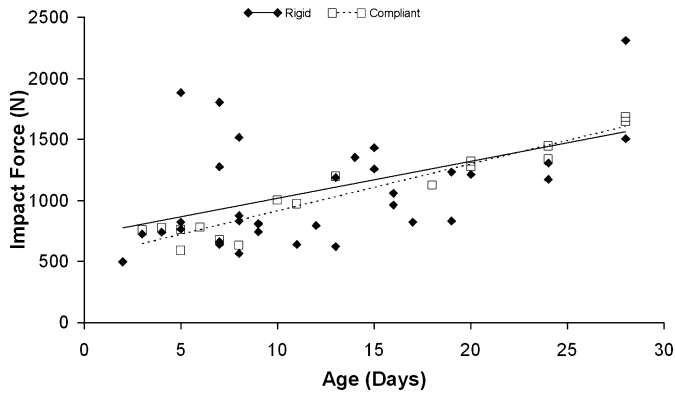


FIG. 3—Peak impact force versus age for both the rigid and compliant interfaces.

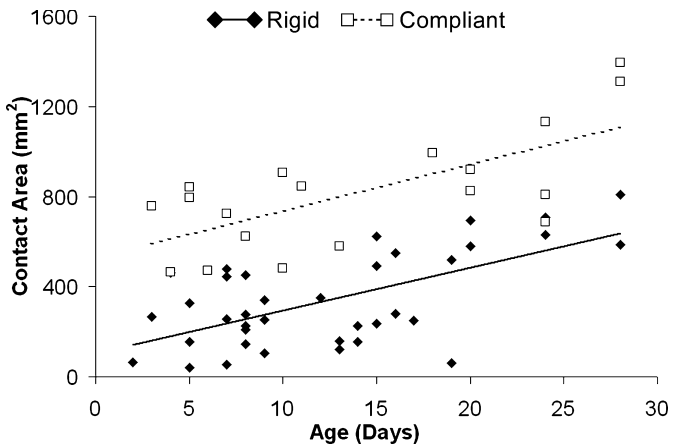


FIG. 4—Impact contact area plotted versus specimen age for both rigid and compliant interfaces.

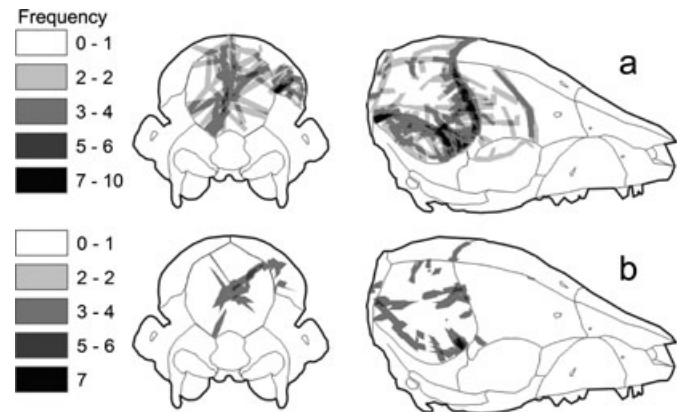


FIG. 6—Geographic Information System map of 2–9 day old rigid (a) and compliant (b) impacts at high energy.

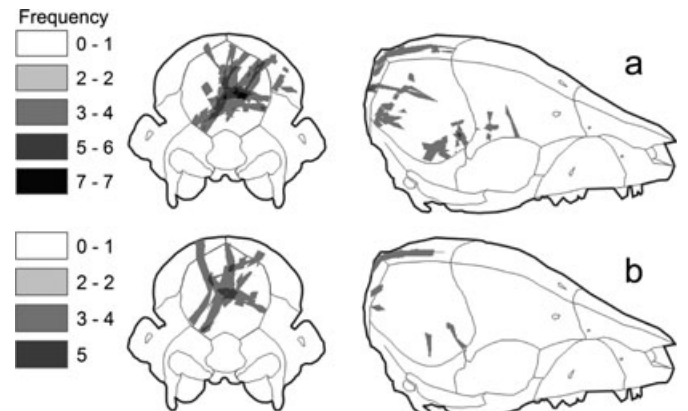


FIG. 7—Geographic Information System map of the 19–28 day old rigid (a) and compliant (b) impacts at high energy.

documented in the younger age group. These sites were also noted in the rigid interface impacts; however, there were more propagated fractures with the rigid interface. Interestingly, in the current study using high energy impacts to the parietal bone, significant fracturing was also documented in the occipital bone for both age groups and interfaces.

The GIS maps of the revisited Baumer et al. (16) data showed three primary areas of fracture initiation, regardless of interface. For the younger age group (2–9 days old), the compliant interface produced more fractures of the skull than the rigid at the same impact energy level (Fig. 8a,b).

For a low energy of impact, there was little to no skull fracture with the compliant interface for the older age group (Fig. 9b). Two fracture initiation sites were noted along the coronal and lambdoid sutures. The rigid impacts produced more propagated fractures initiating at approximately the same locations as in the compliant interface experiments (Fig. 9a).

There were many specimens in both high energy age groups where fractures appeared in the occipital region. These fractures were not present in the revisited Baumer et al. (16) data.

Discussion

The current study focused on skull fracture patterns under a high impact energy as a function of both age and interface using a

porcine model. It was hypothesized that a high level of impact energy would not change the locations of fracture initiation from those documented previously in low energy experiments (16). However, the locations of fracture initiation were found to be a function of impact energy. Baumer et al. (16) document three primary sites of fracture initiation for both interfaces at a low impact energy. While these sites were present in the current study, new initiation sites emerged at the increased level of impact energy. It was also hypothesized in the current study that there would be a greater amount of fracturing via propagation for these higher energy impacts. The amount of fracture produced in the current study was significantly greater than that produced in the low energy experiments conducted by Baumer et al. (16).

An interesting finding in the Baumer et al. (16) study was the equal amount of fracture produced by the rigid and compliant interfaces at c. 18 days of age for a given impact energy. Prior to 18 days, the compliant interface produced more fracture than the rigid interface, but thereafter, there was less for the same impact energy. Baumer et al. (16) suggest that the compliant interface generated higher states of stress near sutures. These stresses were high enough to produce diastatic fractures and therefore a larger amount of total fracture with the compliant interface. In the current study, however, the rigid interface produced more fractures than the compliant interface at all ages, except for the 2-day-old specimens. This change may be attributable to alterations in bone and suture sensitivities to rate of loading. It has been shown in the literature that human bone and suture exhibit mechanical property sensitivities to loading rate (20–22). Young soft tissues, in particular, are more sensitive to changes in loading rate than older tissues (23). Margulies and Thibault (15) also determined that the material properties of young porcine cranial suture at two different rates of loading and documented significant increases in rupture modulus, elastic modulus, and rupture energy at the higher rate. Therefore, at higher rates of loading, sutures may become more “brittle-like,” especially in the younger-aged specimens. The rigid interface may have produced more fractures because of its smaller contact area, which produced higher impact stresses than the compliant interface. Furthermore, with an increase in suture stiffness for these high rates of loading in the current study, higher stresses were likely transmitted across sutures to produce fracture in the occipital bone with both interfaces. These results contrast with the lack of occipital fracture documented in the Baumer et al. (16) study at low levels of impact energy. These findings suggest that high levels of impact energy generate more areas of fracture remote to the impact site.

The greater degree of total skull fracture in the current study was also because of the new sites of fracture initiation with increased levels of impact energy. Baumer et al. (16) documented three primary sites of fracture initiation, regardless of interface (Fig. 8a,b) at low energy. These three sites were also documented in the current study; however, there were one or more additional sites of fracture initiation depending on the interface. One possible explanation for these new sites is the need to dissipate a larger amount of energy through fracture of the bone. In the current study, the initiation sites documented by Baumer et al. (16) were fully propagated through the parietal bone for the rigid interface. Fracture propagation appeared to be one method to dissipate impact energy; however, additional fracture sites were likely needed to allow the bone to dissipate all of the impact energy generated with the higher drop heights in the current study. These new sites were more frequent with the rigid interface because of the impact force being distributed over a smaller area, generating larger impact stresses in the skull. The larger contact area produced with the compliant interface likely attenuated impact stresses resulting in fewer

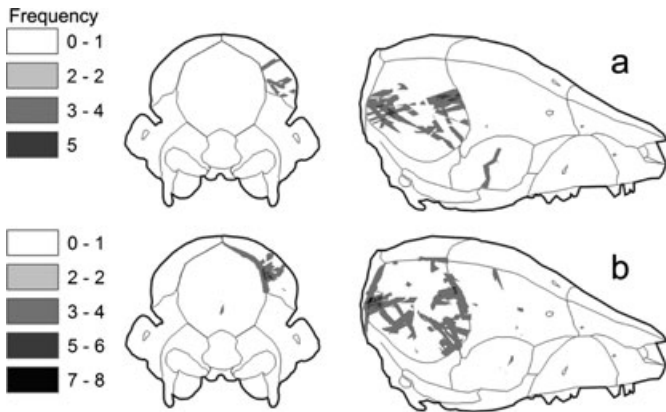


FIG. 8—Geographic Information System map of the 2–9 day old rigid (a) and compliant (b) impacts at low energy.

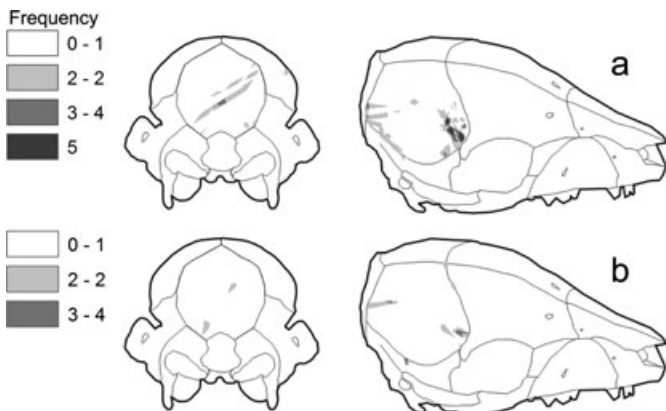


FIG. 9—Geographic Information System map of the 19–28 day old rigid (a) and compliant (b) impacts at low energy.

fracture initiation sites. This difference in fracture initiation sites suggests that the level of impact energy affected a characteristic feature of the fracture pattern for a given interface.

The commonality in fracture patterns for the current and Baumer et al. (16) studies between specimens of the same age and impacted with the same interface was documented using GIS software. This GIS image-analysis approach has been previously used for both archaeological cut-mark distribution on fauna (24) and carnivore modification to faunal remains (25); however, while Damann et al. (26) have examined fracture patterns from human aircraft crashes, this is the first forensic application of the Marean et al. (19) GIS image-analysis technique for bone fracture pattern analysis. Further, this project is unique as it is one of the first attempts to compile fracture pattern data from a relatively large sample of documented experimental impacts. Lee (27) examined fracture patterns of human laryngeal structures after impacting them with a drop tower, but this analysis did not employ GIS, instead using simple tracings of fracture lines. The analyses in the current study provided some insights into the discrimination of fracture characteristics as a function of specimen age, impact interface, and energy for the immature, porcine model. These characteristics were described by assessing the frequency of fracture on each GIS map for the given set of impact conditions. For example, high energy impacts in the younger age group (2–9 days) tended to produce occipital fractures for both interfaces. Again, occipital fracture was not seen in the low energy impacts of Baumer et al. (16).

Additionally, each interface produced characteristic fracture attributes. The rigid interface generated much diastatic fracturing at this higher impact energy, whereas the compliant interface did not. These findings contrast with those noted by Baumer et al. (16), where the compliant interface produced more diastatic fractures than the rigid interface for the younger-aged specimens. One could then say, if a given fracture pattern for a younger-aged specimen involves occipital and diastatic fracture, the causation of injury may well have been a high energy, rigid impact. Future work needs to be focused on the study of uniqueness of these characteristic fracture patterns on the infant porcine skull as a function of impact interface, energy, and specimen age. One limitation of this animal model may be specimen age, as the skull appears to significantly thicken beyond *c.* 24 days of age (data not presented here). A previous study was able to show a good correlation in the development of bending rigidity of the parietal bone using months of human age and days of porcine age up to *c.* 24 days of age (14). And yet, various studies in the current literature have shown that most questions of abusive or accidental trauma involve infants <18 months of age (28).

In cases of infant death via a head injury, the medical examiner faces a difficult task in determining the causation of trauma. Age, interface, and impact energy each appear to affect the pattern and degree of skull fracture in the animal used in this study. Under the impact energy used in the current experiments, the rigid interface produced as much or more skull fracture than the compliant interface at each specimen age. This was in contrast to the previously reported data using lower impact energy with the same animal model, where the compliant interface produced more fractures of the infant porcine skull for specimens <18 days of age (16), but fewer fractures than the rigid interface in more aged specimens. The current study also showed that this higher versus lower level of impact energy as used in our previous study altered the pattern of skull fracture by generating additional sites of fracture initiation in addition to causing propagation of fracture into adjacent, unimpacted bones of the skull. These characteristic fracture patterns were presented as a function of impact energy and interface using GIS software. Future studies will be needed to continue the

characterization of fracture patterns on the immature, porcine skull with the goal of developing mathematical-based algorithms to determine the “best-case” input loading scenario causing specific fracture patterns in this model of the human infant.

Acknowledgments

The authors would like to acknowledge Mr. Ed Reed and Ms. Star Lewis (Reed McKenzie Farms, Decatur, MI) for supplying and collecting the porcine specimens, Ms. Jennifer M. Vollner for technical assistance, and Mr. Cliff Beckett for his technical support.

References

1. Case ME, Graham MA, Handy TC, Jentzen JM, Monteleone JA. Position paper on fatal abusive head injuries in infants and young children. *Am J Forensic Med Pathol* 2001;22:112–22.
2. Billmire ME, Myers PA. Serious head injury in infants: accident or abuse? *Pediatrics* 1985;75:340–2.
3. Reece RM, Sege R. Childhood head injuries: accidental or inflicted. *Arch Pediatr Adolesc Med* 2000;154:11–5.
4. Wheeler DS, Shope TR. Depressed skull fracture in a 7-month old who fell from bed. *Pediatrics* 1997;100:1033–4.
5. Hobb CJ. Skull fracture and the diagnosis of abuse. *Arch Dis Child* 1984;59:246–52.
6. Meservy CJ, Towbin R, McLaurin RL, Myers PA, Ball W. Radiographic characteristics of skull fractures resulting from child abuse. *Am J Roentgenol* 1987;149:173–5.
7. Leventhal JM, Thomas SA, Rosenfield NS, Markowitz RI. Fractures in young children: distinguishing child abuse from unintentional injuries. *Am J Dis Child* 1993;147:87–92.
8. Bertocci GE, Pierce MC, Deemer E, Aguel F, Janosky JE, Vogeley E. Using test dummy experiments to investigate pediatric injury risk in simulated short-distance falls. *Arch Pediatr Adolesc Med* 2003;157(5):480–6.
9. Knight B. Forensic pathology. London, UK: Edward Arnold, 1991.
10. Cooperman DR, Merten DF. Skeletal manifestation of child abuse. In: Reece RM, Ludwig S, editors. *Child abuse: medical diagnosis and management*. Philadelphia, PA: Lippincott, Williams and Wilkins, 2001;123–56.
11. Prange MT, Luck JF, Dibb A, Van Ee CA, Nightingale RW, Myers BS. Mechanical properties and anthropometry of the human infant head. *Stapp Car Crash J* 2004;48:279–99.
12. Pierce M, Valdevit A, Anderson L, Inoue N, Hauser D. Biomechanical evaluation of dual-energy x-ray absorptiometry for predicting fracture loads of the infant femur for injury investigation: an in vitro porcine model. *J Orthop Trauma* 2000;14(8):571–6.
13. Herring S, Teng S. Strain in the braincase and its sutures during function. *Am J Phys Anthropol* 2000;112:575–93.
14. Baumer TG, Powell BJ, Fenton TW, Haut RC. Age dependent mechanical properties of the infant porcine parietal bone and a correlation to the human. *J Biomech Eng* 2009;131(11):1–6.
15. Margulies SS, Thibault KL. Infant skull and suture properties: measurements and implications for mechanisms of pediatric brain injury. *J Biomech Eng* 2000;122(4):364–71.
16. Baumer TG, Passalacqua NV, Powell BJ, Newberry WN, Fenton TW, Haut RC. Age-dependent fracture characteristics of rigid and compliant surface impacts on the infant skull—a porcine model. *J Forensic Sci* 2010;55(4):993–7.
17. Stewart G, Meert K, Rosenberg N. Trauma in infants less than three months of age. *Pediatr Emerg Care* 1993;9(4):199–201.
18. Atkinson PJ, Newberry WN, Atkinson TS, Haut RC. A method to increase the sensitive range of pressure sensitive film. *J Biomech* 1998;31(9):855–9.
19. Marean CW, Abe Y, Nilssen PJ, Stone EC. Estimating the minimum number of skeletal elements (MNE) in zooarchaeology: a review and a new image-analysis GIS approach. *Am Antiq* 2001;66(2):333–48.
20. Wood J. Dynamic response of human cranial bone. *J Biomech* 1971;4(1):1–12.
21. Yoganandan N, Pintar FA, Sances A, Walsh PR, Ewing CL, Thomas DJ, et al. Biomechanics of skull fracture. *J Neurotrauma* 1995;12(4):659–69.

22. Motherway JA, Verschueren P, Van der Perre G, Sloten JV, Gilchrist MD. The mechanical properties of cranial bone: the effect of loading rate and cranial sampling position. *J Biomech* 2009;42(13):2129–35.
23. Haut RC. Age-dependent influence of strain rate on the tensile failure of rat-tail tendon. *J Biomech Eng* 1983;105(3):296–9.
24. Abe Y, Marean CW, Nilssen PJ, Assefa Z, Stone EC. The analysis of cutmarks on archaeofauna: a review and critique of quantification procedures, and a new image-analysis GIS approach. *Am Antiq* 2002;67(4):643–63.
25. Hodgson JA, Plummer TW, Forrest F, Bose R, Oliver JS. A GIS-based approach to documenting large canid damage to bones. Proceedings of the 79th Annual Meeting of the American Association of Physical Anthropologists; 2010 April 14-17; Albuquerque, New Mexico, 2010;129.
26. Damann FE, Adler R, Benedix DC, Kontanis EJ. Patterns of perimortem fracture from military aircraft crashes. Proceedings of the 60th Annual Meeting of the American Academy of Forensic Sciences; 2008 Feb 18–23; Washington, DC; 2008;324–5.
27. Lee SY. Experimental blunt injury to the larynx. *Ann Otol Rhinol Laryngol* 1992;101(3):270–4.
28. Kemp A, Dunstan F, Harrison S, Morris S, Mann M, Rolfe K, et al. Patterns of skeletal fractures in child abuse: systematic review. *BMJ* 2008;337:1–8.

Additional information and reprint requests:
 Roger C. Haut, Ph.D.
 Orthopaedic Biomechanics Laboratories
 A-407 East Fee Hall
 Michigan State University
 East Lansing, MI 48824
 E-mail: haut@msu.edu